Correcting X-ray Spectra obtained from the AXAF VETA - I Mirror Calibration for Pileup, Continuum, Background and Deadtime.

G. Chartas, K. Flanagan, J. P. Hughes, E. M. Kellogg, D. Nguyen, M. Zombeck
Center for Astrophysics
60 Garden Street
Cambridge,MA 02138

M. Joy and J. Kolodziejezak
Space Science Laboratory
George C. Marshall Space Flight Center
Huntsville, AL 35812

Abstract

The VETA-I mirror was calibrated with the use of a collimated soft X-ray source produced by electron bombardment of various anode materials. The FWHM, effective area and encircled energy were measured with the use of proportional counters that were scanned with a set of circular apertures. The pulsers from the proportional counters were sent through a multichannel analyzer that produced a pulse height spectrum. In order to characterize the properties of the mirror at different discrete photon energies one desires to extract from the pulse height distribution only those photons that originated from the characteristic line emission of the X-ray target source.

We have developed a code that fits a modeled spectrum to the observed X-ray data, extracts the counts that originated from the line emission, and estimates the error in these counts. The function that is fitted to the X-ray spectra includes a Prescott function for the resolution of the detector a second Prescott function for a pileup peak and a X-ray continuum function. The continuum component is determined by calculating the absorption of the target Bremsstrahlung through various filters, correcting for the reflectivity of the mirror and convolving with the detector response.

Introduction

The VETA-I (Verification Engineering Test Article-I) consists of a pair of Wolter Type-I mirrors which are intended to be used as the outermost set of the AXAF (Advanced X-ray Astrophysical Facility) telescope. A detailed description of the performance and scientific advances anticipated from AXAF observations are listed in reference[1]. The improved sensitivity of the AXAF mirrors compared with those of the Einstein and ROSAT X-ray telescopes results mainly from the larger attainable effective area of AXAF over a broader energy bandwidth and the higher angular resolution resulting from improvements in the mirror figure and surface smoothness. A natural consequence of these improvecents is the need to use detectors with higher spatial and energy resolution and the need to employ more sophisticated data reduction techniques. The physical properties of the VETA-I optic measured are the FWHM, the effective area and encircled energy. Definitions of these quantities are given in Kellogg et al[2]. For the initial analysis of the VETA-I proportional counter spectra we used a quick-look analysis technique which basically involved the summation of counts in a selected region of interest. The quick-look data provided a fair description of most of the mirrors properties with a moderate amount of analysis. In this paper we will describe a more elaborate method for analyzing the VETA-I data which leads to a determination of the mirror effective area to better than 5% and the encircled energy better than 2%. In our analysis we will apply a set of corrections for the spectral contamination of the measured proportional counter data due to the existence of a bremsstrahlung component in the X-ray source, pulse pileup effects which distort the spectrum, background and deadtime.

In section 1 we provide a brief outline of the experimental setup. A detailed description of the model employed for the data reduction is given in section 2. Finally section 3 is devoted to the presentation of the results of the VETA-I data reduction and a discussion of the effect of these corrections on the measured mirror properties.

1. 0 The VETA-I calibration set up

The VETA-I calibration set-up is shown in figure 1. An electron impact X-ray source with interchangeable targets and filters is located 528 m away from the optic in order to approximate an incident plane wave. The parabola P1 and hyperbola H1 mirrors are made out of zerodur and were supported by flexures. Their relative alignment and centering were adjusted with a set of linear actuators. The X-ray flux incident on the VETA-I

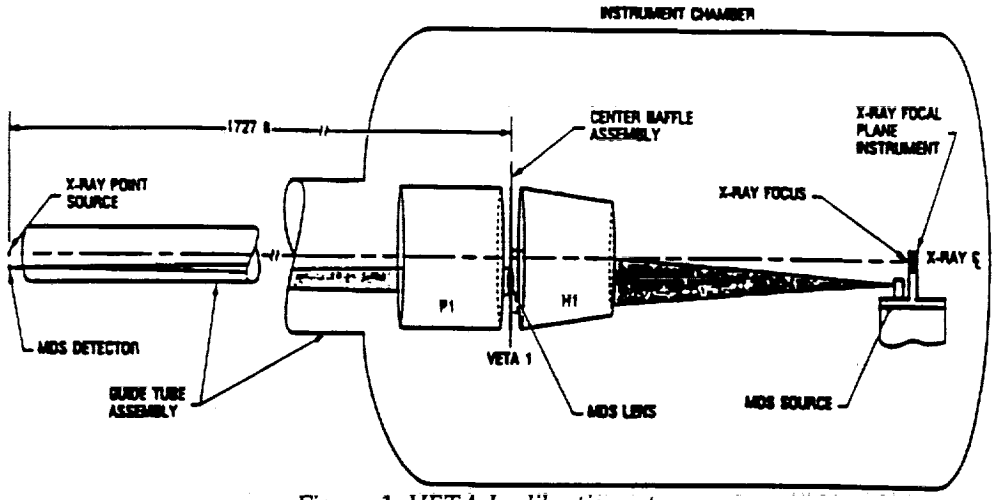

Figure 1. *VETA-I calibration set up*

was monitored by sealed and flow proportional counters manufactured by LND Inc. while an identical pair of sealed and flow counters were located at the focal plane of the VETA approximately 10 meters behind the optic. The flow counters have a graphite coated 1.7 μm thick polypropylene window. For energies below 1.49 keV the flow counters were filled with methane at a pressure of 250 Torr while for energies above 1.49 keV a mixture of 90% Ar and 10% methane (P10) at a pressure of 400 Torr was used. The electronics associated in acquiring the data are shown in figure 2. A set of periodic pulsers (not shown in the figure) were injected into 2 multichannel analyzer (MCA) channels in order to monitor the deadtime of the pulse height system. The focused X-ray image was scanned by translating a plate containing a set of pinholes, slits and annuli across the image with a position accuracy of approximately 1 μm.

2.0 Model of the VETA-I monitor and focal plane proportional counter spectra

The description of our model will trace the sequence of events traced by X-ray photons as they are produced through the deceleration of electrons in various targets, transmitted through filters to minimize the bremsstrahlung component, reflected by the P1-H1 mirrors and finally absorbed inside a proportional counter. The resulting pulses are fed into a multichannel analyzer which converts their relative pulse height to a channel address.

2.1 X-ray source spectrum

For the analysis of the VETA-I data we have adopted Kramers relationship for the bremsstrahlung emission of the soft X-ray source:

$$I(E) = kZ(E_{max} - E) \qquad (1)$$

where E_{max} is the high voltage of the source anode, Z is the atomic number of the target and k is a fitted parameter with units of inverse energy. The spectra that we obtained from the beam monitor detectors allow a direct fit to the continuum component at energies above the characteristic X-ray lines.

2.2 Transmission of source filters and counter windows

In section 2.6 we will show that one of the main contributors to the error in the derived focal plane (XDA) and beam monitor detector (BND) events is the continuum component under the line peak. In order to minimize the bremsstrahlung intensity under the peak a source filter is used with an absorption edge slightly higher in energy than the characteristic line. The properties of the source filters used in the VETA-I test are shown in table (1). The errors quoted by the manufactures are near 30% and are due to errors in the measuring technique. The effective source filter thickness is the thickness determined by fitting a ensemble of BND spectra and performing a grid search of filter thickness vs. the ensemble average χ^2 as shown in figure 3. The 68.3% confidence level is just χ^2_{min} (unreduced) +1. Similarly an ensemble of BND spectra are fitted in order

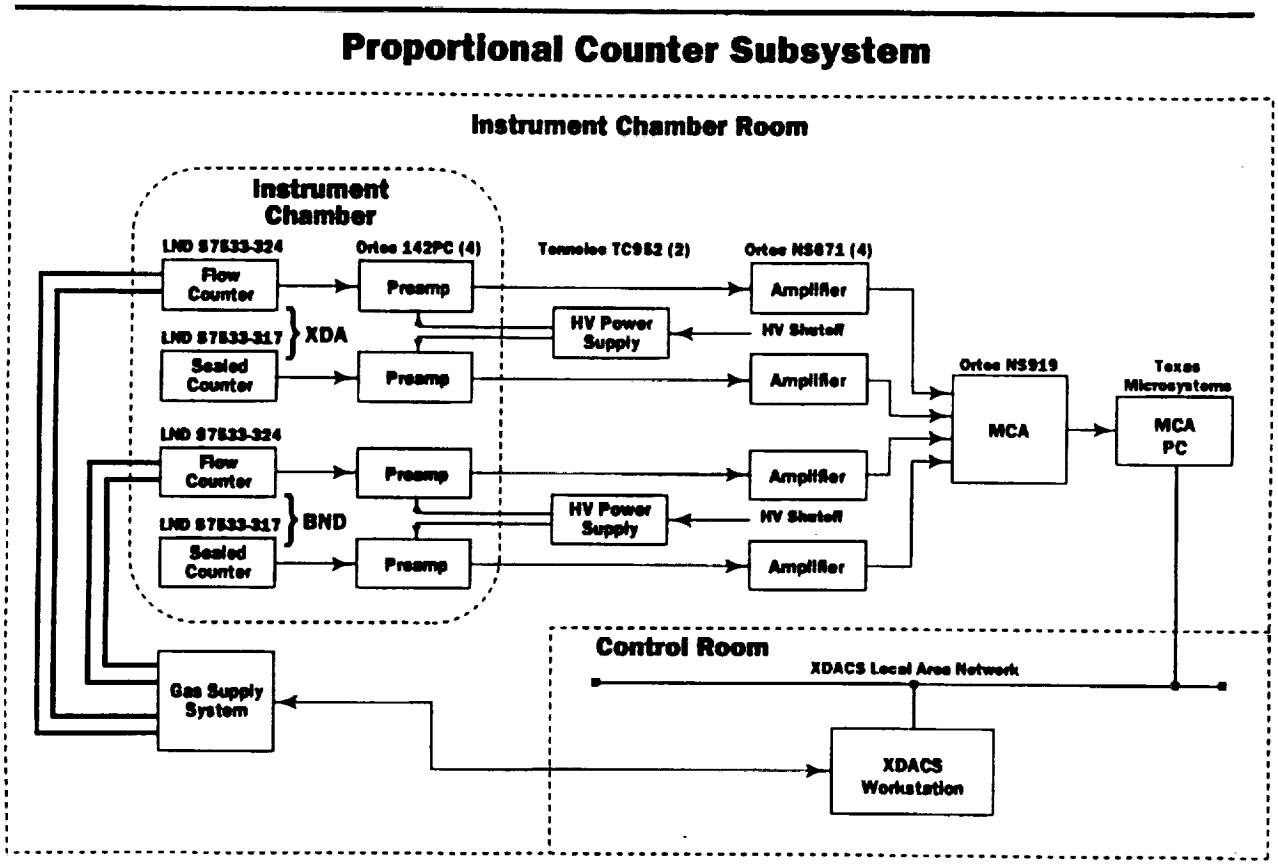

Figure 2. *Proportional counter electronics*

to determine the strength of line and continuum emission of the X-ray source.

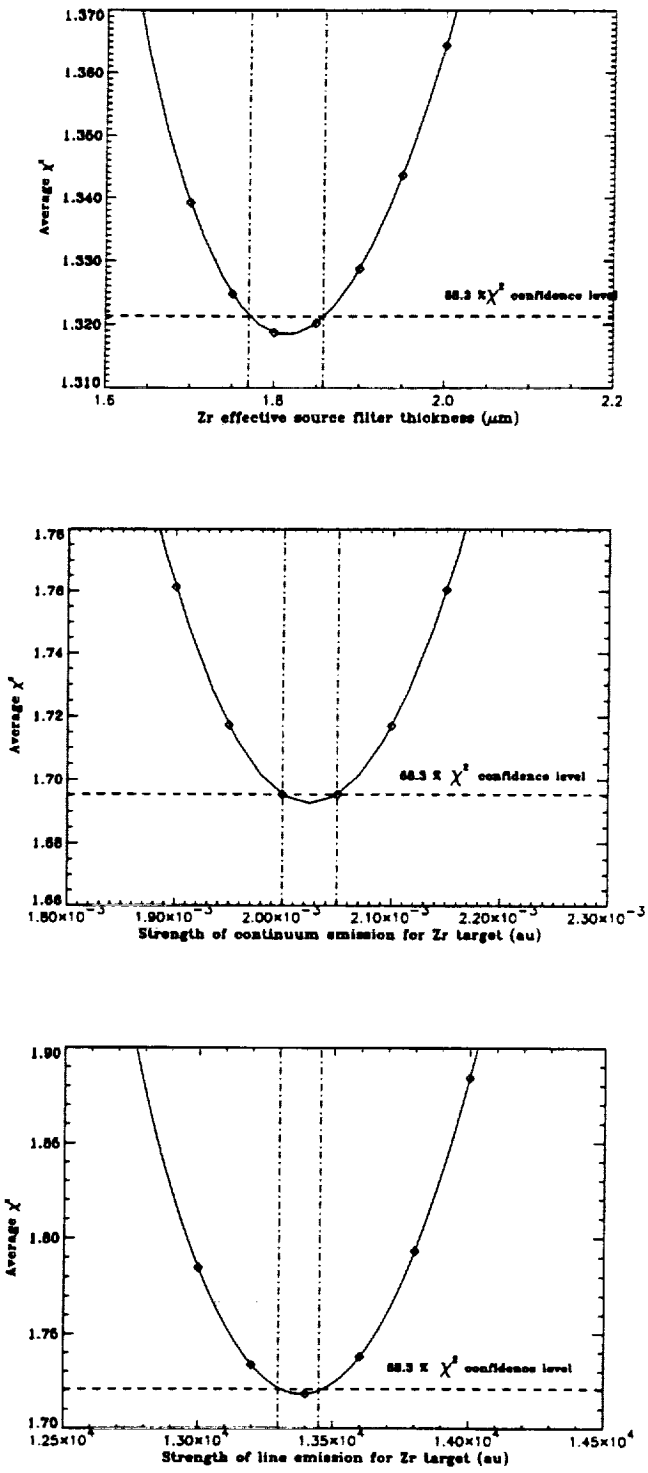

Figure 3. χ^2 *grid search for source filter thickness, line strength and continuum strength*

The ratio of the effective thickness to the nominal value for the thicknesses ranged between 0.9 for Zr and approximately 2.6 for Mo. An independent measurement of the Mo thickness performed in a post VETA test provided similar results for the effective filter thickness and strongly suggests an error in the labeled Mo nominal filter thickness.

Table 1:

Source filters	Nominal Thickness ρd_n	Effective filter thickness ρd_{eff}
Parylene	2.20×10^{-4} gr cm^{-2}	$(1.7 \pm 0.1) \times 10^{-4}$ gr cm^{-2}
Al	2.70×10^{-3} gr cm^{-2}	$(2.8 \pm 0.1) \times 10^{-3}$ gr cm^{-2}
Mo	2.04×10^{-3} gr cm^{-2}	$(5.36 \pm 0.05) \times 10^{-3}$ gr cm^{-2}
Zr	1.29×10^{-3} gr cm^{-2}	$(1.17 \pm 0.03) \times 10^{-3}$ gr cm^{-2}
Cu	4.48×10^{-4} gr cm^{-2}	$(5.82 \pm 0.5) \times 10^{-4}$ gr cm^{-2}

2.3 Resolution, efficiency and uniformity of proportional counters used in the VETA-I calibration

The resolution function R(E) of a proportional counter provides the response of a counter for an incident monoenergetic beam of X-rays of energy E. Various resolution functions have been determined theoretically by studying the statistics of secondary electrons produced by the primary photoelectrons and the multiple electron avalanches initiated by each secondary electron. For energies above 2 keV the response can be approximated with a Gaussian with a mean proportional to the energy and a FWHM proportional to $E^{1/2}$. This approximation breaks down however at low energies where one observes an asymmetry in the response. This is mainly due to the small number n of avalanches produced per secondary electron (n = the energy of the electron / ionization energy) and consequently for low energies one does not expect, according to the central limit theorem, to obtain a Gaussian distribution.

For the present analysis the resolution of the proportional counter is approximated by a function first derived by Prescott[3] which takes into account the statistics of multiple avalanches. The Prescott function has the form:

$$F(x) = \frac{N\left(\frac{m}{x}\right)^{3/4}}{\sqrt{4\pi m Q}} exp\left(2\sqrt{\frac{mx}{Q^2}} - \frac{(m+x)}{Q}\right) \qquad (2)$$

where the mean $\bar{x}$ of the distribution is $\bar{x} = m/Q^2$ and the standard deviation is $\sigma = \sqrt{2mQ}$, Q is the Prescott

width parameter. By minimizing the Prescott function F(x), $\frac{d}{dx}F(x) = 0$, one can derive the following relationship between the mean and the width parameter:

$$\frac{m}{x_{max}} = 1 + \frac{3}{2}\frac{Q}{x_{max}} + \frac{9}{16}\frac{Q^2}{x^2_{max}} \quad (3)$$

In our algorithm the m and Q parameters of the line component of the spectrum are fitted parameters. For the determination of the measured continuum component one requires to know the width parameter vs. energy in order to convolve the detector response with the modeled incident continuum component over the measured energy band.

By fitting a range of X-ray lines we have produced an empirical expression for Q(E) for E in the range of 0 to 2.5 keV:

$$Q(E) = a_0E + a_1E^2 + a_2E^3 + a_3E^4 \quad (4)$$

with a_0 = 0.08514, a_1 = -0.13751, a_2 = 0.08026, a_3 = -0.01552

The measured energy resolution and Prescott Q parameter for the proportional counters used in the VETA test are shown in figure 4.

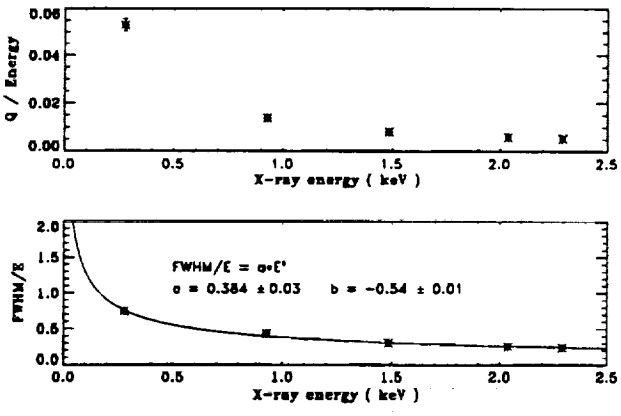

Figure 4. *Measured Prescott Q parameter and proportional counter energy resolution*

2.4 Peak pileup correction

Soft X-ray spectra obtained during the VETA -I calibrations show evidence of peak pileup at high counting rates. Each pileup count corresponds to 2 events that were not separately detected in the multichannel analyzer. At energies below the 1.49 keV Al line the poor detector energy resolution does not allow a direct determination of the pileup component. The pileup peak represents a small distortion to the spectrum and is corrected for by performing a simultaneous fit to the line and pileup peak. This fit provides a relation between the percent pileup counts and the total event rate. The measured pileup versus total event rate is shown in figure 5.

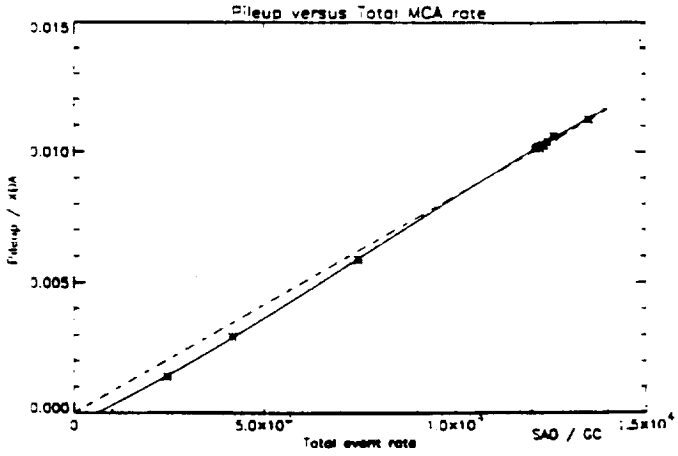

Figure 5 *Measured pileup rate vs. total MCA event rate*

We have compared our results to a theoretical model presented in Johns and Yaffe[4] which predicts that the percent pileup follows the equation:

$$\frac{N_{pu}}{N_{XDA}} = (1. - e^{-2\rho\tau}) \quad (5)$$

where N_{XDA} are the total number of focal plane events originating from the X-ray line, N_{pu} are the photon events that are piled up, ρ is the average photon event rate (from all MCA channels) and τ is the characteristic time of the MCA. The theoretical prediction is also shown in figure 5. The fitted value for τ is 1.85e-7 sec. The measured pileup fraction f(ρ) is fit to a 3'rd degree polynomial:

$$f(\rho) = b(1)\rho + b(2)\rho^2 + b(3)\rho^3$$

where b(1) = 4.845e-7, b(2) = 5.876e-11, b(3) = -2.441e-15

2.5 Extraction of X-ray line counts

The function that describes the model fitted to the focal plane spectrum has the form:

$$f_{XDA}(i) = f_{line}(i) + f_{cont}(i) + f_{pu}(i) + f_{bgd}(i) \qquad (6)$$

where $f_{XDA}(i)$ are the counts in the MCA pulse height channel i, f_{line} is the X-ray line component which includes all excited K and L lines and their escape peaks and is attenuated by the mirror reflectivity, f_{cont} is the continuum part of the spectrum which also contains the fluorescence radiation that escapes the counter and the effect of the mirror reflectivity, f_{pu} is the pileup component and f_{bgd} is the normalized for live time background. In the calculation of the continuum and line component we perform a convolution of the detector response $R(E_i,E_j)$ with the incident X-ray spectrum. The incident spectrum is a sum of nl X-ray lines of strength a_1*s(Ej), where s(Ej) is the relative intensity of line Ej obtained from reference[5], and a bremsstrahlung emission $Brem(E_k)$ of strength a_2. For the focal plane spectrum we include the effect of reflectance off the mirror by multiplying with the model effective area $A(E_j)$ as determined by ray tracing the P1-H1 mirror surface and using Henke 90 optical constants for zerodur. The input model effective area of the VETA-I is shown in figure 6 together with the energies at which the calibration was performed.

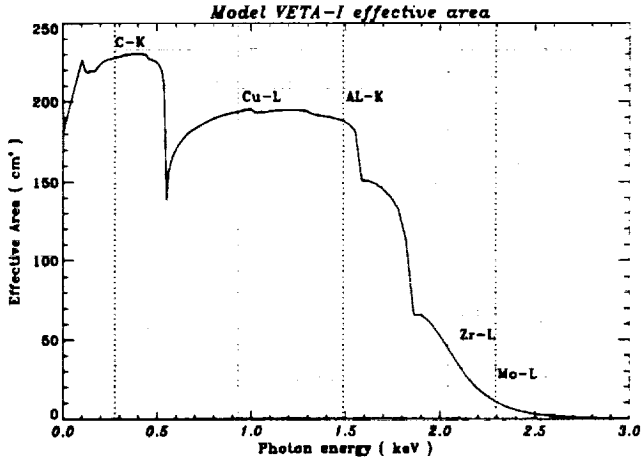

Figure 6. *Input model effective area of the VETA-I*

The line component of equation (6) is calculated by using the expression:

$$f_{line}(i) = a_1 \sum_{j=1}^{nl} s(E_j) T_f(E_j) T_w(E_j) Abs(E_j) A(E_j)$$
$$\times [\ (1 - esc(E_j, E_l))\, R(E_i, E_j) +$$
$$+ esc(E_j, E_l)\, R(E_i, E_j - E_l)\ ]$$

For the continuum component we used:

$$f_{cont}(i) = a_2 \sum_{k=1}^{ph} T_f(E_k) T_w(E_k) Abs(E_k) Brem(E_k)$$
$$\times [\ (1 - esc(E_k, E_l))\, R(E_i, E_k) +$$
$$+ esc(E_k, E_l)\, R(E_i, E_k - E_l)\ ]$$

T_f and T_w are the transmission of the source filter and counter window respectively, $Abs(E_j)$ is the efficiency of the counter, $esc(E_i,E_j)$ is the probability of a fluorescence photon of energy E_i escaping from the counter times the fluorescence yield.

The background component is normalized to take into account differences in the live time between the background run and the test run. $f'_{bgd}(i)$ is the measured background MCA spectrum.

$$f_{bgd}(i) = \frac{t_{int} \times (1 - dt_{bgd})}{t_{bgd}(1 - dt_{MCA})} f'_{bgd}(i)$$

were t_{int} is the integration time, t_{bgd} is the integration time of the background run, dt_{bgd} and dt_{MCA} are the deadtime of the background run and test run respectively.

For extracting the counts that originated from the X-ray line emission we begin by fitting the model function of equation (6) to the spectrum using a Marquardt nonlinear least squares routine. We select a region of interest (ROI), determined by the XDA MCA channels (m_0,m_1) and BND MCA channels (n_0,n_1), around the line peak and sum the measured pulse height counts. We then subtract the fitted continuum component in the ROI, subtract the pileup in the ROI, add the fitted line counts outside the ROI, add two times the total pileup counts (every pileup count corresponds to two events detected as one count) and finally subtract the normalized background counts. The extracted line counts for the focal plane detector $XDA_{p,c,b}$, corrected for pileup, continuum and background effects, are given by the expression:

$$XDA_{p,c,b} = \sum_{i=m_0}^{m_1} S_{XDA}(i) + \sum_{i=0}^{m_0 - 1} f_{line}(i) + \qquad (7)$$

$$+\sum_{i=m_1+1}^{m_{max}} f_{line}(i) + 2. \times N_{pu} - \sum_{i=m_0}^{m_1} f_{pu}(i) -$$

$$-\sum_{i=m_0}^{m_1} f_{cont}(i) - \frac{t_{int} \times (1. - dt_{bgd})}{t_{bgd} \times (1. - dt_{XDA})} f_{bgd}$$

The extracted line counts for the beam monitor detector $BND_{c,d}$, corrected for continuum and background are:

$$BND_{c,d} = \sum_{i=n_0}^{n_1} S_{BND}(i) + \sum_{i=0}^{n_0-1} f_{line}(i) + \quad (8)$$

$$+\sum_{i=n_1+1}^{n_{max}} f_{line}(i) - \sum_{i=n_0}^{n_1} f_{cont}(i) -$$

$$-\frac{t_{int} \times (1. - dt_{bgd})}{t_{bgd} \times (1. - dt_{BND})} f_{bgd}$$

where $S_{XDA}(i)$ and $S_{BND}(i)$ are the counts in pulse height channel i from the total focal plane and beam monitor proportional counter spectra, dt_{XDA} and dt_{BND} are the deadtime in the MCA channels that contain the XDA and BND spectra respectively.

The BND count rate is significantly lower than the XDA count rate and pileup effects are less than 0.1% and for this reason we have not included a pileup correction for the beam monitor spectra.

2.6 Error analysis implemented in spectral extraction

The objective of the VETA-I calibration was to measure the encircled energy with 2% precision and the effective area to 5%. In the present analysis we will present the calculated 1 σ error components of the measured effective area that are due to fitting errors, pileup effects, bremsstrahlung, continuum, background subtraction and the deadtime correction. We now proceed in propagating errors through equations (7) and (8) that give the focal plane and beam monitor line events, in terms of the corresponding quantities in counts and percent deadtime.

$$\sigma^2_{XDA_{d,p,c,b}} = \sigma^2_{XDA_{d,p,c}} \left(\frac{1}{1 - dt_{XDA}}\right)^2 + \quad (9)$$

$$+\sigma^2_{dt_{XDA}} \left[\frac{XDA_{p,c,b}}{(1 - dt_{XDA})^2}\right]^2$$

Subscripts d,p,c and b to a quantity refer to deadtime, pileup, continuum and background corrections to that quantity. $XDA_{p,c,b}$ are the counts in the XDA spectrum originating from line emission and corrected for pileup, continuum and background. The error contributions from each effect can be seen in the following equations where we have neglected errors in the deadtime for the background, which contributes less than 0.05%. The error in the focal plane counts is:

$$\sigma^2_{XDA_{p,c,b}} = \sum_{i=m_0}^{m_1} S_{XDA}(i) + \sum_{i=0}^{m_0-1} f_{line}(i) +$$

$$+\sum_{i=m_1+1}^{m_{max}} f_{line}(i) + 4. \times \sigma^2_{pu} + \sigma^2_{pufit} + \quad (10)$$

$$+\sigma^2_{f_{cont}} + \left(\frac{t_{int} \times (1. - dt_{bgd})}{t_{bgd} \times (1. - dt_{XDA})}\right)^2 \times \sum_{i=m_0}^{m_1} f_{bgd}(i)$$

For the error in the beam monitor counts we neglect the pileup terms due to the relatively low count rates measured in the BND detector.

$$\sigma^2_{BND_{c,b}} = \sum_{i=n_0}^{n_1} S_{BND}(i) + \sum_{i=0}^{n_0-1} f_{line}(i) + \quad (11)$$

$$\sum_{i=n_1+1}^{n_{max}} f_{line}(i) + \sigma^2_{f_{cont}} +$$

$$\left(\frac{t_{int} \times (1. - dt_{bgd})}{t_{bgd} \times (1. - dt_{XDA})}\right)^2 \times \sum_{i=n_0}^{n_1} f_{bgd}(i)$$

σ_{pu} is the standard deviation in the pileup counts, σ_{pufit} is the standard deviation of the pileup counts in the region of interest (m_0,m_1). The errors due to the deadtime correction are:

$$\sigma^2_{dt_{XDA}} = \left(\frac{\sum_{i=m_4}^{m_5} S_{XDA}(i) - \sum_{i=m_2}^{m_3} S_{XDA}(i)}{t_{int} \times f^2_{p1}} \right)^2 \sigma^2_{fp1} +$$

$$+ \left(\frac{1}{t_{int} \times f_{p1}}\right)^2 \times \left((0.289)^2 + \sum_{i=m_3}^{m_4} S_{XDA}(i) \right)$$

$$\sigma^2_{dt_{BND}} = \left(\frac{\sum_{i=b_4}^{n_5} S_{BND}(i) - \sum_{i=b_2}^{n_3} S_{BND}(i)}{t_{int} \times f^2_{p2}} \right)^2 \sigma^2_{f_{p2}} +$$

$$\left(\frac{1}{t_{int} \times f_{p2}}\right)^2 \times \left((0.289)^2 + \sum_{i=n_3}^{n_4} S_{BND}(i) \right)$$

The pulse height channels over which the pulser counts appear in the XDA and BND MCA spectra are (m_4,m_5) and (n_4,n_5) respectively. Since the pulser used for the deadtime correction was periodic, the error in the pulser counts as measured in the MCA is :

$$\sqrt{\int_0^1 (x-\mu)^2 P(x)\, dx} = 0.289 \text{ counts}$$

while the error in the injected pulser rate is : $f_p = 0.289/t_{pulser}$, where t_{pulser} is the time over which pulser rate is measured.

The errors in determining the continuum component from the fit are:

$$\sigma^2_{f_{cont,XDA}} = \sum_{j=0}^{np} \left[\sigma_{a(j)} \frac{\partial}{\partial a(j)} \sum_{i=m_0}^{m_1} f_{cont,XDA}(i) \right]^2$$

$$\sigma^2_{f_{cont,BND}} = \sum_{j=0}^{np} \left[\sigma_{b(j)} \frac{\partial}{\partial b(j)} \sum_{i=n_0}^{n_1} f_{cont,BND}(i) \right]^2$$

The summations are performed over the np variables (a(j) for the XDA spectrum and b(j) for the BND spectrum) of the continuum component; source filter thickness, line strength, continuum strength, the Q Prescott parameter of the detector response, the m Prescott parameter and the model scaling factor.

3.0 Results and discussion

In figure 7 we present fits and their residuals to the beam monitor and focal plane spectra for Al, Zr,C and Mo source targets. The continuum component for the carbon spectrum was measured in a post VETA test where the proportional counter gain was set appropriately such that the high energy continuum could be fitted. A set of apertures with pinhole diameters ranging from 5 μm to 20 mm were placed at the focal plane in front of the XDA proportional counter in order to measure the encircled energy at different radii.The calculated encircled energy using both quick look and fitting techniques are presented in figure 8. The difference between encircled energy calculated by each method is very noticeable for Zr and Mo.This can be explained by referring to the model effective area of the mirror in figure 6. Notice that near Zr the effective area curve is very steep. This implies that the attenuation of the continuum component in the XDA spectrum will be strongly dependent on energy, resulting in a line to continuum ratio in the region of interest quite different from the one measured in the BND spectrum.

Since the largest error component in determining the line counts in a spectrum originates from the continuum subtraction one desires to minimize the continuum counts in the ROI by selecting a ROI as small as possible around the X-ray line peak. Obviously for detectors with better energy resolution one may select narrower ROI's thus reducing the error due to the continuum subtraction. We have investigated the sensitivity of the calculated line events in the spectrum with the selected region of interest and found that it is insignificant. The variation of the calculated encircled energy with selected region of interest for both the quick look analysis technique and the spectral fitting technique is shown in figure 9. Notice that the quicklook analysis technique is very sensitive to the selected region of interest. Initial values for the effective area used in the fit to the focal plane spectra were obtained by ray tracing the VETA-I mirror and using optical constants as measured by Henke et al. The next iterative step is to repeat the analysis using the effective area as determined from the fits to the spectra as input to the code.

In table 2 we present the measured 1 sigma uncertainties in the XDA and BND line events. The error in the ratio XDA/BND at a certain energy reflects the measured uncertainty in determining the encircled energy (EE) at that energy, since the EE for our experimental setup is approximately π x XDA/BND.

The energy scale of the pulse height channels is also determined with an iterative procedure. We initially locate the pulse height channel that corresponds to the peak of the smoothed spectrum. This value is used as an initial guess for the fitting routine which after a certain number of iterations provides the pulse height channel that corresponds to the maximum of the fitted line component of the spectrum. The pulse height

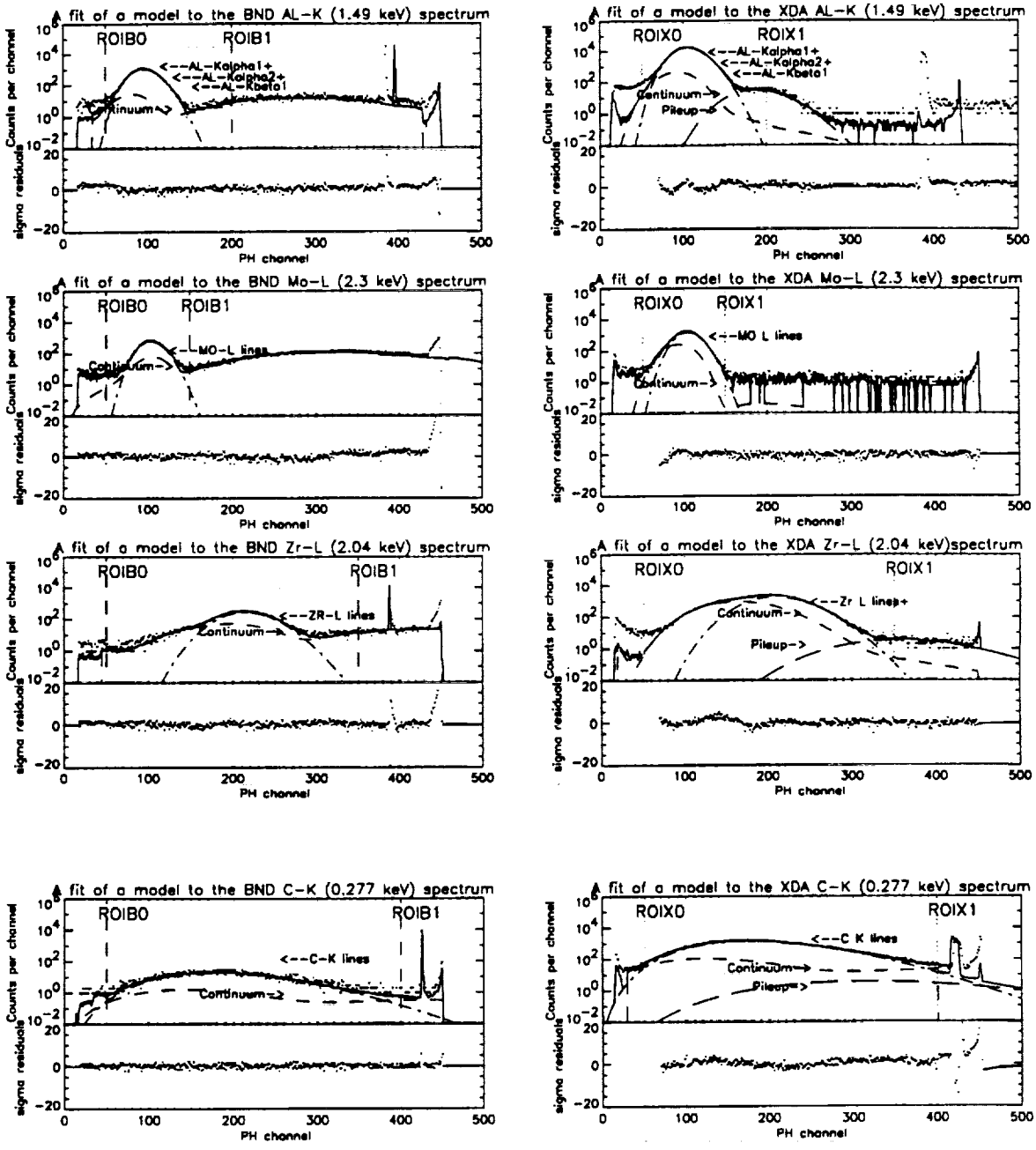

Figure 7. *Fits and residuals of a model to Al,Zr,Mo and C VETA-I spectra*

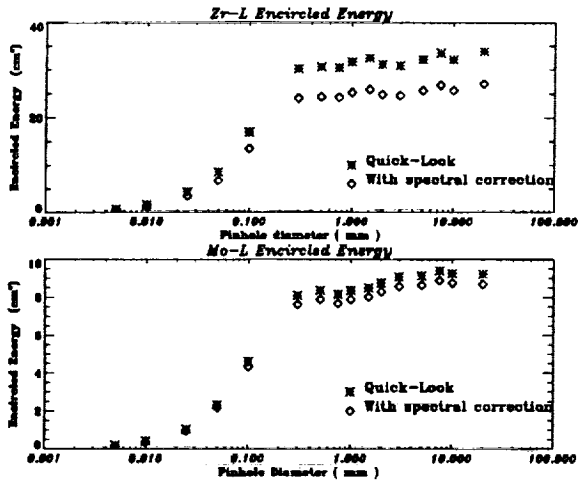

Figure 8. *Measured encircled energy using both quick-look and fitting techniques*

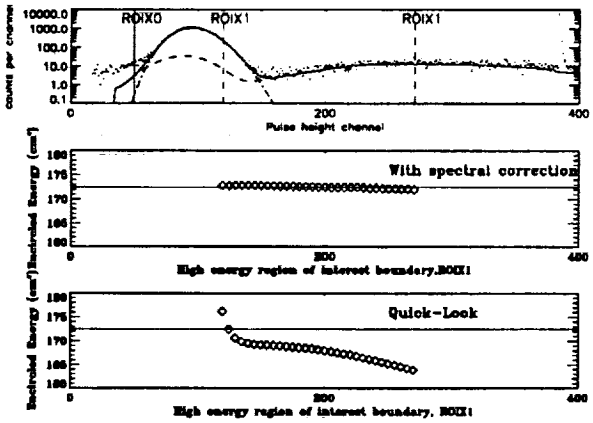

Figure 9. *Variation of the measured encircled energy with selected region of interest for both the quick look analysis technique and the spectral fitting technique*

energy scale is then recalculated using the corrected value for the line peak location. This procedure is especially effective when dealing with low count spectra and spectra with large continuum components.

The effects of X-ray transmission attenuation due to the proportional counter window mesh are treated in a separate paper by Zhao et al[6].

Table 2: Measured 1 sigma uncertainties in the XDA and BND line events

	C	Cu	Al	Zr	Mo
σ_{XDA}	0.37%	0.2%	0.17%	0.53%	0.68%
σ_{BND}	0.20%	1.1%	0.15%	0.66%	1.2%
$\sigma_{\frac{XDA}{BND}}$	0.42%	1.2%	0.23%	0.85%	1.4%

Acknowledgments

We would like to acknowledge Dan Schwartz, Diab Jerius and Ping Zhao for useful conversations. The work reported here has been supported in part by NASA Contract NAS8 - 36123

References

1. Astro. Lett. and Communications, 1987, Vol. 26

2. Kellogg et al, SPIE 1992, this conf.

3. J. R. Prescott, " *Photomultiplier single-electron statistics and the shape of the ideal scintillation line."* Nuc. Ins. and Meth. 22 1963.

4. P. C. Johns and M. J. Yaffe,"*Correction of pulse height spectra for peak pileup effects using periodic and random pulse generators.*" Nuc. Ins. and Meth. A225 1987.

5. S. I. Salem, S. L. Panossian and R. A. Krause,"*Experimental K and L relative X-ray emission rates.*"- Atomic Data and Nuclear Data Tables 14, 1974.

6. Zhao et al, SPIE 1992 , this conf.